DOT/FAA/AM-05/14
Office of Aerospace Medicine
Washington, DC 20591

Solar Radiation Alert System

Kyle Copeland[1]
Herbert H. Sauer[2]
Wallace Friedberg[1]

[1]Civil Aerospace Medical Institute
Federal Aviation Administration
Oklahoma City, OK 73125

[2]CIRES, University of Colorado and
National Geophysical Data Center
NOAA, Boulder, CO 80305

July 2005

Final Report

U.S. Department of Transportation
Federal Aviation Administration

NOTICE

Technical Report Documentation Page

1. Report No.	2. Government Accession No.	3. Recipient's Catalog No.
DOT/FAA/AM-05/14		

4. Title and Subtitle	5. Report Date
Solar Radiation Alert System	July 2005
	6. Performing Organization Code

7. Author(s)	8. Performing Organization Report No.
Copeland K,[1] Sauer HH,[2] Friedberg W[1]	

9. Performing Organization Name and Address		10. Work Unit No. (TRAIS)
[1]FAA Civil Aerospace Medical Institute P.O. Box 25082 Oklahoma City, OK 73125	[2]CIRES, University of Colorado & National Geophysical Data Center NOAA, Boulder, CO 80305	11. Contract or Grant No.

12. Sponsoring Agency Name and Address	13. Type of Report and Period Covered
Office of Aerospace Medicine Federal Aviation Administration 800 Independence Ave., S.W. Washington, DC 20591	14. Sponsoring Agency Code

15. Supplemental Notes
This work was accomplished under the approved tasks TOXLAB.AV9000.

16. Abstract
A solar radiation alert (SRA) system has been developed to continuously evaluate measurements of high-energy protons made by instruments on Geosynchronous Operational Environmental satellites. If the measurements indicate the likelihood of a substantial elevation of effective dose rates at aircraft flight altitudes, the Civil Aerospace Medical Institute issues an SRA to the aviation community via the National Oceanic and Atmospheric Administration Weather Wire Service. This report describes the methodology of the SRA system. A Monte Carlo particle transport code was used to estimate the fluences of secondary particles (protons, neutrons, pions, kaons, photons, electrons, and muons) in selected energy ranges at specific altitudes. Coefficients to convert particle fluence to effective dose incorporate radiation-weighting factors and tissue-weighting factors recommended by the International Commission on Radiological Protection, except that the radiation-weighting factor for protons was changed from five to two, as recommended by the National Council on Radiation Protection and Measurements. Effective dose rates from solar-proton-induced ionizing radiation in the earth's atmosphere at high geomagnetic latitudes were calculated for the solar proton event of 20 January 2005. The event started at 06:50 Universal Time, and within 5 minutes, dose rates at 60,000, 40,000, and 30,000 ft (relative to mean sea level) reached maximum values of: 140, 55, and 21 microsieverts per hour, respectively.

17. Key Words	18. Distribution Statement
Solar Radiation, Monte Carlo Particle Transport Code, Solar Protons, Solar Particles, Space Weather, Solar Flare, Coronal Mass Ejection	Document is available to the public through the Defense Technical Information Center, Ft. Belvior, VA 22060; and the National Technical Information Service, Springfield, VA 22161

19. Security Classif. (of this report)	20. Security Classif. (of this page)	21. No. of Pages	22. Price
Unclassified	Unclassified	13	

Form DOT F 1700.7 (8-72) Reproduction of completed page is authorized

ACKNOWLEDGMENTS

For editorial and technical contributions to this report, we thank: E.B. Darden, Jr., Oak Ridge Associated Universities (Ret.), Oak Ridge, Tennessee; M.E. Wayda and F.E. Duke, Civil Aerospace Medical Institute, FAA, Oklahoma City, Oklahoma; D.E. Parker, University of Oklahoma Health Sciences Center, Oklahoma City, Oklahoma; and M.A. Shea and D. F. Smart, University of Alabama, Huntsville, Alabama.

SOLAR RADIATION ALERT SYSTEM

INTRODUCTION

Aircraft passengers and crew are constantly exposed to ionizing radiation at higher dose rates than normally received by the general population. The principal ionizing radiation is galactic cosmic radiation, a main source of which is believed to be supernovae (exploding stars). Occasionally, a disturbance in the sun (solar flare, coronal mass ejection) leads to a large flux of solar protons with sufficient energy to penetrate the earth's magnetic field, enter the atmosphere, and increase ionizing radiation levels at aircraft flight altitudes. For a primer on aircrew exposure to ionizing radiation, see report by Friedberg and Copeland (1).

A system (Figure 1) has been developed for the continuous evaluation of proton flux measurements made by instruments on Geosynchronous Operational Environmental Satellites (GOES). At present, the primary data source is GOES-11 while GOES-10 measurements are used if they are more current or if GOES-11 is not operating properly. If the measurements indicate the likelihood of a substantial elevation of ionizing radiation levels at aircraft flight altitudes at high latitudes, the Civil Aerospace Medical Institute (CAMI) issues a Solar Radiation Alert (SRA) to the National Oceanic and Atmospheric Administration Weather Wire Service (NWWS) (2). Information given with the alert includes estimated dose rates in microsieverts per hour (μSv/h), based on 5-minute averages, at 30,000, 40,000, 50,000, 60,000, and 70,000 ft (relative to mean sea level). The dose rates are updated at 5-minute intervals for the duration of the SRA.

The specific criteria for issuance of an SRA are that the estimated effective dose rates induced by solar protons at any altitude from 30,000 to 70,000 ft in the earth's atmosphere are equal to or greater than 20 microsieverts per hour for each of three consecutive 5-minute periods. The three 5-minute periods need not be at the same altitude. Because of the potential for a delay of 3 to 20 minutes in communication processes and the three 5-minute periods, notification of the start of SRA conditions may be 18 to 35 minutes after the start of the first 5-minute period. Possible effects on the dose rate caused by ions other than protons (e.g., alpha particles) in the primary solar particle flux, shielding by the earth's magnetic field, and shielding by aircraft structure are not taken into account in the calculations. The SRA is canceled when the average effective dose rate at all altitudes from 30,000 to 70,000 ft is less than 20 microsieverts per hour for six consecutive 5-minute periods.

METHOD USED TO ESTIMATE EFFECTIVE DOSE RATES AT FLIGHT ALTITUDES

Basis of SRA System

The Primary Solar Proton Spectrum. Observations of fluxes of high-energy protons used to estimate solar radiation dose rates in the earth's atmosphere are obtained from GOES proton flux measurements. These measurements are recorded in several "channels": P4 to P7 (15 to 900 MeV energy, 168 to 1581 MV rigidity), P10 (510 to 700 MeV, 1103 to 1343 MV), and P11 (greater than 700 MeV, greater than 1343 MV). Protons in channels P4 through P10 are in terms of differential flux (particles/cm^2/steradian/second/MeV). Protons in channel P11 are in terms of integral flux (particles/cm^2/steradian/second).

The proton fluxes currently available from the Space Environment Center (SEC) are derived from satellite-instrument count rates using conversion factors appropriate for GOES-7 instruments (3). In Steps 1 to 3, below, these fluxes are converted to count rates and then reconverted to flux using the conversion factors specifically intended for GOES-10 and GOES-11. Channels P8 and P9 are excluded from the analysis because their correction algorithms are more complex than those of the other channels, and excluding them does not significantly affect the calculated dose rates.

The data are available in near real-time from the file transfer protocol (ftp) server at the SEC and are also on the Internet (4). Protons flux observations are from solar plus galactic cosmic radiation. The contribution of galactic protons is subtracted from the total as part of the correction process described below. The initial 5-minute average galactic background count rate (B, counts/second) for a channel is the average of the preceding 12 hours of data (144 5-minute periods) collected when no solar particle event or Forbush decrease (sudden reduction in galactic background radiation as a result of scattering of low-energy galactic particles by magnetic fields

carried by solar particles) is occurring. Once the system is operating, the background is changed as described in Step 10, below.

In each channel, solar protons of sufficiently high energy to cause an increase in ionizing radiation levels in the atmosphere have a flux spectrum *(f)* across the channel's energy acceptance band that can reasonably be expressed as a power law function of rigidity *(R)*:

$$f(R) = \alpha R^{-\gamma} \qquad \text{(Eq. 1)}$$

where the proton spectrum is characterized in terms of time-dependent constants, intensity (α) and spectral hardness index (γ) (5,6). Six spectra in the form of Eq.1, each spanning a different rigidity range, are created in Steps 1 to 7 (below) using GOES data.

These six spectra are combined in Step 8 to form a complete spectrum used to calculate effective doses in Step 9. A piecewise-continuous spectrum is needed because during solar proton events, γ increases at higher rigidities.

Radiation Transport. Monte Carlo radiation transport code MCNPX2.4.0 (7) was used to calculate the fluences (particles/cm^2) of secondary particles (protons, neutrons, pions, kaons, photons, electrons, and muons) in selected energy ranges for specific altitudes, which were generated by mono-energetic isotropic fluences of protons at an altitude of 100 km. Solar proton fluences at 100 km were assumed to be isotropic because there is no directional information in the GOES data. The atmospheric pressure density at 100 km is 0.0003 g/cm^2. Using a higher altitude to more closely approximate the free-space environment of the satellite would not significantly improve dose estimates. The earth was modeled as a sphere of liquid water with a radius of 6371 km and a density of 1g/cm^3. The atmosphere was modeled as a series of 100 spherically symmetric 1-km thick layers surrounding the earth. The composition (a gaseous mixture containing nitrogen, oxygen, argon, and carbon atoms) and density of each layer were assumed to be that reported for the middle of the layer (8), resulting in an atmosphere with a vertical depth of 1035.08 g/cm^2. Altitudes in Table 1 were calculated from the atmospheric depth. Geomagnetic effects were neglected.

Fluence-to-Effective Dose Conversion. With one exception, fluence-to-effective-dose conversion coefficients reported by Pellicioni (9) were used to convert the secondary particle fluences generated by the transport code to effective doses. The reported coefficients incorporate radiation-weighting factors and tissue-weighting factors recommended by the International Commission on Radiological Protection. The one exception is the radiation-weighting factor for protons, which was changed from five to two, as recommended by the National Council on Radiation Protection and Measurements (10). The effective dose from kaons was not calculated because its contribution to the total dose would have been negligible. Table 1 shows, at selected altitudes, the dose rate per unit flux of primary solar protons of selected rigidities. The transport code automatically converts a fluence below 10^{-25} particles/cm^2 to zero fluence, which would lead to a zero dose rate per unit flux (Table 1). To avoid this, any zero dose rate per unit flux was changed from zero to $1\text{x}10^{-12}$. Table 1, as presented, is applicable to any solar particle event.

Calculating Effective Dose Rate at Specific Altitudes

Step 1. Convert the incorrect fluxes obtained from the SEC to instrument count rates (*C*), by multiplying the flux (φ) for each channel used (φ_{P4}, φ_{P5}, φ_{P6}, φ_{P7}, φ_{P10}, and φ_{P11}) by the appropriate conversion factor (*k*) from Table 2:

$$C = \varphi k \qquad \text{(Eq. 2)}$$

GOES-10 and GOES-11 have identical instruments and therefore use the same conversion factors.

Step 2. Subtract the galactic background count rate *(B)* from the total count rate (*C*, galactic plus solar) to obtain the solar-induced count rate (*C′*):

$$C' = C - B \qquad \text{(Eq. 3)}$$

If *C′* is negative, assign it a value of 1% of *B*. Calculation of *B* is described earlier, in the section entitled "The Primary Solar Proton Spectrum."

Step 3. Divide the background corrected solar count rate (*C′)* by the appropriate conversion factor *(k′)* from Table 2 to obtain the differential flux *(f(R))*:

$$f(R) = C'/k' \qquad \text{(Eq. 4)}$$

Step 4. Calculate a preliminary spectral hardness index (γ) for each pair *(i,j)* of channels (P4 and P5, P5 and P6, P6 and P7, P7 and P10, P10 and P11) using Eq. 5, which was derived from Eq. 1:

$$\gamma_{Pi,Pj} = \frac{\ln(f(R)_{Pi}) - \ln(f(R)_{Pj})}{\ln(R_{Pj}) - \ln(R_{Pi})} \qquad \text{(Eq. 5)}$$

Variables $f(R)_{P4}$ through $f(R)_{P11}$ are differential proton fluxes derived from values in channels P4 through P11 (Steps 1 to 3). The characteristic rigidities of the protons in these channels are R_{P4} through R_{P11} from Table 2.

Step 5. Further correct the differential fluxes $(f(R)_{Pi})$, using spectral hardness index correction factors(s) in Table 3:

$$f(R)_{corrected} = f(R)\,s \qquad \text{(Eq. 6)}$$

Use the $\gamma_{Pi,Pj}$ values from Step 4 to find the appropriate s values. Thus, use $\gamma_{P4,P5}$ to find the s value to correct $f(R)_{P4}$, use $\gamma_{P5,P6}$ to find the s value to correct $f(R)_{P5}$, etc. This selection procedure weights the spectral response towards the higher energies. $f(R)_{P11}$ does not require this correction.

Step 6. Recalculate γ values with Eq. 5, using fluxes $f(R)_{Pi}$ and $f(R)_{Pj}$ that were corrected in Step 5. If γ is negative, assign it the value 0. If γ equals 1, assign it the value 1.000001.

Step 7. Calculate α for each channel with Eq. 7 using the characteristic rigidities from Table 2, the differential fluxes $f(R)_{corrected}$ from Step 5, and the recalculated γ values from Step 6:

$$\alpha = f(R)_{corrected}/R^{-\gamma} \qquad \text{(Eq. 7)}$$

with $f(R)_{P4}$ use $\gamma_{P4,P5,}$ with $f(R)_{P5}$ use $\gamma_{P5,P6}$, etc. For channel P11, use the α found for P10. Convert channel P11 count rate *(C′)* to integral flux (F_{P11}), irrespective of γ, by dividing C' by its geometric factor 0.73 (3). Use Eq. 8 to find the γ that best describes F_{P11}. Start with γ equal to $\gamma_{P10,P11}$ and, if necessary, decrease γ in steps of 0.000001 until the relationship is just satisfied.

$$F_{P11} \le \int_{1343MV}^{32545MV} \alpha\, R^{-\gamma} dR \qquad \text{(Eq. 8)}$$

The upper and lower limits in Eq. 8 are the rigidity bounds set for channel P11. The upper limit is the upper rigidity limit of the Monte Carlo calculations, 32545 MV (Table 1), and the lower limit is 1343 MV, the lowest rigidity of data in P11.

Step 8. Construct a piecewise-continuous description of the solar proton spectrum *(ψ(R))* for primary solar protons with rigidities above 137 MV (10 MeV) based on results of Steps 1 to 7, with each piece having the form of Eq. 1. With the exception of the upper rigidity limit of channel P11, the upper and lower rigidity limits used with the parameters calculated for each channel are shown in Table 4. The upper rigidity limit for channel P11 (and thus for *ψ(R))* is R_{max} and is found by replacing the upper rigidity limit in Eq. 8 with 1344 MV, then increasing the upper limit in steps of 1 MV until the relationship is just satisfied.

Step 9. For a specific altitude *(H)*, the effective dose rate per unit flux of primary solar protons (Δ*(R,H))* is generated from the data in Table 1. For intermediate R values, Δ*(R,H)* is generated using linear interpolation of Log*(R)* and Log(Δ*(R,H))*. Primary solar protons in bins with rigidities less than 183.5 MV (17.78 MeV), the lowest rigidity in Table 1, are assigned the same Δ*(R,H)* as primary solar protons of 183.5 MV. The effective dose rate *(E(H)*, microsieverts per hour) at a particular altitude is the integral

$$E(H) = \int_{R_{min}}^{R_{max}} \psi(R)\Delta(R,H)\,dR \qquad \text{(Eq. 9)}$$

where R_{min} is the lower limit of channel P4 (Table 4) and R_{max} is from Step 8. The numerical integration is performed using 1 MV-wide flux bins. For each bin, the Δ*(R,H)* value used is the mean of the Δ*(R,H)* values at the extreme rigidities of the bin.

Dose rates at altitudes between those listed in Table 1 are estimated using a cubic spline interpolation.

Step 10. If C from Step 2 does not exceed twice B in any channel, C is used to update B in each channel:

$$B = (143B + C)/144 \qquad \text{(Eq. 10)}$$

Thus, the background count rates will always be the averages of the last 12 uneventful hours.

To examine solar proton events using proton flux data from satellites other than the current GOES series (GOES-8, GOES-9, GOES-10, GOES-11, GOES-12), minor modifications are necessary: any satellite data set may be used that allows the reasonable construction of a solar proton spectrum spanning the rigidity range 137 MV to above 1343 MV.

RESULTS AND DISCUSSION

In estimating dose rates for the SRA system, only solar protons are used because they are the dominant contributor to the ionizing radiation from the sun at aircraft flight altitudes and data are available in near real-time. Other radiation information, such as GOES alpha particle measurements and data from the worldwide network of neutron monitors, would enable more complete calculations, but not with the immediacy required of an alert system.

During the early stages of a solar proton event (solar particle event where the proton flux with energies equal to or greater than 10 MeV exceeds 10 particles/second/steradian/cm^2 (11)), solar radiation in the vicinity of the earth is usually somewhat anisotropic, as indicated by ground-level neutron monitor data (12). However, anisotropy is not particularly evident in GOES data. The

15 largest solar proton events from 1996 through 2003 for which data were available from two or more satellites were examined to compare event onset times and flux measurements. Apparent event onset times at the satellites were the same (within 5 minutes). The largest differences in fluxes measured by the satellites, typically 20%, were observed at energies greater than 350 MeV during the first few 5-minute periods of an event. As the event proceeded, differences decreased. Longitudinal separation of the most widely separated satellites was about 60 degrees. The low anisotropy effects observed at the satellites indicate that doses generated by the system are reasonable first estimates at aircraft flight altitudes at polar latitudes (i.e., where the cutoff rigidity is close to 0 MV).

Figure 2 shows effective dose rates from solar protons in the earth's atmosphere during the solar proton event of 20 January 2005. The calculations do not take into account geomagnetic shielding (i.e., shielding by the earth's magnetic field) and shielding by aircraft structure. Inclusion of aluminum shielding afforded aircraft occupants in a B-747 (using a skin thickness of 0.6 g/cm^2), for example, would not change the effective dose estimates at 40,000 ft by more than a few percent (depending on the specific energy spectrum, the effective dose could increase or decrease). The event started at 06:50 Universal Time (UT), and by 06:55 UT dose rates at 60,000, 40,000, and 30,000 ft had reached maximum values of: 140, 55, and 21 microsieverts per hour, respectively. The dose rates then dropped rapidly: at 07:55 UT, they were 17, 4, and 1 microsieverts per hour at the three altitudes.

The SRA system provides timely, quantitative information for the aviation community on potentially hazardous solar radiation levels at aircraft flight altitudes in high-latitude regions. This information enables users to decide whether or not reducing aircraft flight altitudes is appropriate.

Future work includes: (a) improve estimates of dose rates in Table 1 by improving Monte Carlo calculations, (b) improve estimates of radiation levels at neutron monitor locations by including geomagnetic and anisotropy effects on dose rates, (c) possible incorporation of dose rates from alpha particles and any other significant heavier ions in the solar particle flux, and (d) calculation of dose rates, flight doses, and neutron monitor counting rates during past solar proton events.

REFERENCES

1. Friedberg, W., and Copeland, K. What Aircrews Should Know About Their Occupational Exposure to Ionizing Radiation. Washington, DC: U.S. Department of Transportation, Federal Aviation Administration, Office of Aerospace Medicine, Technical Report no. DOT/FAA/AM-03/16 (2003). Available through the National Technical Information Service, Springfield, VA 22161 and at: http://www.faa.gov/library/reports/medical/oamtechreports/2000s/media/0316.pdf (date accessed: 7 July 2005). This publication and all Office of Aerospace Medicine technical reports are available in full-text from the Civil Aerospace Medical Institute's publications Web site: http://www.faa.gov/library/reports/medical/oamtechreports/

2. National Weather Service. Solar Radiation Alerts are distributed to subscribers of the NOAA Weather Wire Service (NWWS). The NWWS is administered for the National Weather Service by DynCorp Systems and Solutions, LLC; 1500 Conference Center Drive, Chantilly, VA 20151-3808, phone: (703) 818-4000.

3. Sauer, H.H. Analysis of GOES Particle Data and the Development of a Processing Procedure in Support of FAA Requirements for Radiation Exposure Estimation at Aircraft Altitudes, Boulder, CO: CIRES/NOAA-NGDC (2003). Prepared for the FAA under contract number DTFA0201P09198. 6973H5 FAA Aero Center AMQ-300. Appendix C contains the instrument manufacturer's calibration report "Calibration Report for the EPS DOME Sensor Response to Protons" NXT-CAL-102, May 30, 1995, Panametrics, Inc. for Space Systems/Loral, Inc. The FAA contracted report is in the library of the Civil Aerospace Medical Institute, Oklahoma City, OK.

4. National Oceanic and Atmospheric Administration, Space Environment Center Web site: http://www.sec.noaa.gov/ftpmenu/lists/pchan.html. Files to select are G11pchan_5m.txt and G10pchan_5m.txt (date accessed: 7 June 2005).

5. Ellison, D.C. and Ramaty, R. Shock Acceleration of Electrons and Ions in Solar Flares. The Astrophysical Journal 298: 400-408 (1985).

6. Brown, J.C., Smith, D.F., and Spicer, D.S. Solar Flare Observations and Their Interpretations. In The Sun as a Star, Jordan, S. (Ed./Author), Washington, DC: National Aeronautics and Space Administration Science and Technical Information Branch, Technical Report no. NASA SP-450, pp. 81-227 (1981).

7. Los Alamos National Laboratory. Monte Carlo N-Particle Transport Code System for Multiparticle and High Energy Applications (MCNPX 2.4.0), released August 2002. Available from the Radiation Safety Information Computational Center at the Oak Ridge National Laboratory.

8. National Oceanic and Atmospheric Administration, National Aeronautics and Space Administration, and United States Air Force. U.S. Standard Atmosphere, 1976. NOAA S/T 76-1562, Washington, DC: U.S. Government Printing Office (1976).

9. Pellicioni, M. Overview of Fluence-to-Effective Dose and Fluence-to-Ambient Dose Equivalent Conversion Coefficients for High Energy Radiation Calculated Using the FLUKA Code. Radiation Protection Dosimetry 88(4): 279-297, (2000).

10. National Council on Radiation Protection and Measurements. Limitation of Exposure to Ionizing Radiation. NCRP Report No.116 (p. 20, Table 4.3) (1993).

11. National Oceanic and Atmospheric Administration, Space Environment Center Web site: http://sec.noaa.gov/tiger/SolarProtons.html (date accessed: 6 June 2005).

12. Smart, D.F. and Shea, M.A. The Local Time Dependence of the Anisotropic Solar Cosmic Ray Flux. Advances in Space Research 32(1): 109-114 (2003).

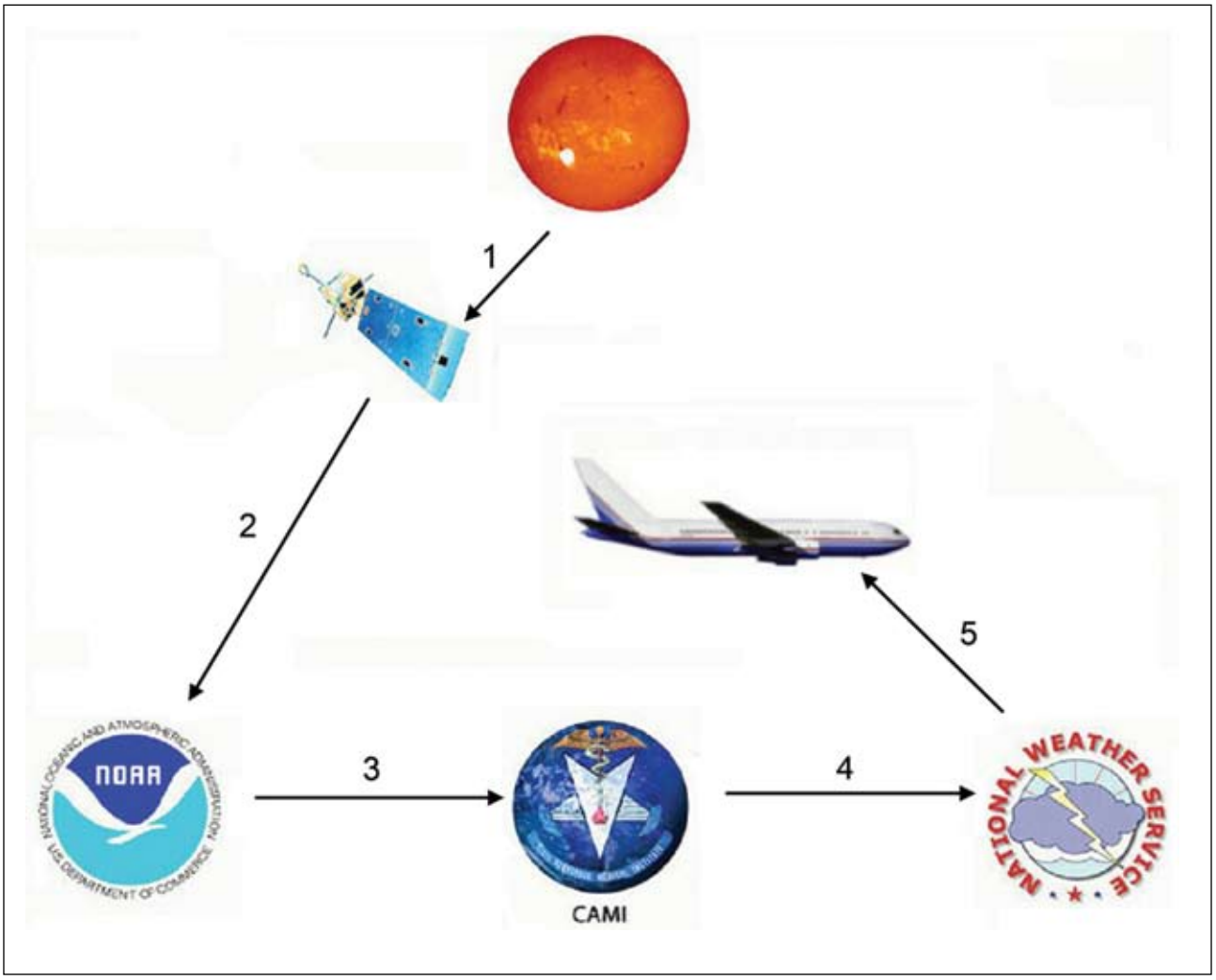

Figure 1. Solar radiation alert system: (1) Occasionally, a disturbance in the sun (solar flare, coronal mass ejection) leads to a large flux of high-energy particles in the vicinity of the earth. (2) Instruments on a GOES satellite continuously measure the radiation and the information is transmitted to NOAA. (3) From there it is sent to CAMI. A computer at CAMI analyzes the measurements. (4) If the measurements indicate the likelihood of a substantial elevation of ionizing radiation levels at aircraft flight altitudes, a Solar Radiation Alert is issued to the NOAA Weather Wire Service within 10 minutes. (5) NOAA Weather Wire Service subscribers are provided estimated effective dose rates for 30,000, 40,000, 50,000, 60,000, and 70,000 ft. This information is updated at 5-minute intervals for the duration of the alert.

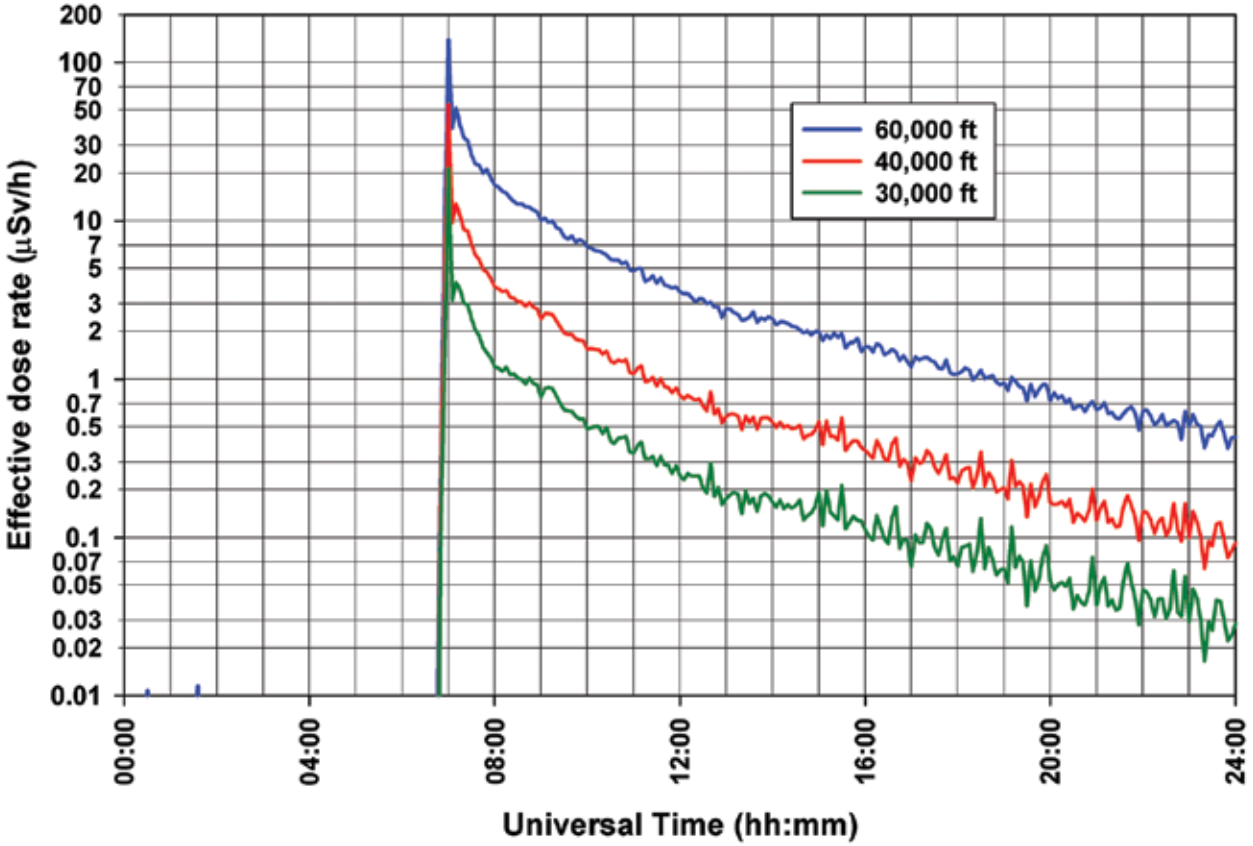

Figure 2. Effective dose rates from solar proton-induced ionizing radiation at selected altitudes on 20 January 2005 (based on GOES-11 data, geomagnetic effects neglected).

Table 1. Effective dose rate per unit flux of primary solar protons, as related to incident rigidity and energy at selected altitudes in the atmosphere relative to mean sea level.

		Dose rate per unit flux, $\Delta(R,H)$, microsieverts per hour/(protons/cm^2/steradian/second) at altitude (H) [a]			
Rigidity (R), MV	Energy, MeV	H= -50 ft	H=9722 ft	H=19,588 ft	H=29,378 ft
183.5	17.78	1.000×10^{-12}	1.000×10^{-12}	1.000×10^{-12}	2.901×10^{-9}
245.6	31.62	1.000×10^{-12}	1.000×10^{-12}	1.404×10^{-10}	1.256×10^{-8}
329.7	56.23	1.000×10^{-12}	1.000×10^{-12}	2.978×10^{-9}	2.063×10^{-7}
444.6	100	1.000×10^{-12}	9.739×10^{-9}	2.251×10^{-7}	7.796×10^{-6}
604.4	177.8	9.040×10^{-8}	1.919×10^{-7}	7.713×10^{-6}	1.271×10^{-4}
832.7	316.2	5.281×10^{-7}	2.489×10^{-5}	2.935×10^{-4}	1.960×10^{-3}
1171.	562.3	7.556×10^{-6}	2.383×10^{-4}	2.267×10^{-3}	1.207×10^{-2}
1696.	1000	4.294×10^{-5}	1.122×10^{-3}	9.903×10^{-3}	5.130×10^{-2}
2549.	1778	2.173×10^{-4}	4.428×10^{-3}	3.625×10^{-2}	0.1469
3991.	3162	7.719×10^{-4}	1.495×10^{-2}	9.106×10^{-2}	0.3009
4848.	4000	1.122×10^{-3}	1.915×10^{-2}	0.1147	0.3651
6495.	5623	1.885×10^{-3}	2.356×10^{-2}	0.1319	0.4335
10898.	10000	7.433×10^{-3}	4.966×10^{-2}	0.2413	0.7315
18695.	17780	2.202×10^{-2}	0.1064	0.4464	1.277
20917.	20000	2.751×10^{-2}	0.1227	0.5025	1.410
32545.	31620	6.046×10^{-2}	0.2178	0.7942	2.110
	H=39,197 ft	H=48,977 ft	H=58,749 ft	H=68,511 ft	H=78,260 ft
183.5	8.348×10^{-8}	1.282×10^{-6}	7.556×10^{-6}	1.937×10^{-5}	3.215×10^{-5}
245.6	9.257×10^{-7}	1.521×10^{-5}	7.390×10^{-5}	1.699×10^{-4}	2.622×10^{-4}
329.7	1.199×10^{-5}	1.223×10^{-4}	4.873×10^{-4}	1.004×10^{-3}	1.456×10^{-3}
444.6	1.511×10^{-4}	7.832×10^{-4}	2.407×10^{-3}	4.436×10^{-3}	6.602×10^{-3}
604.4	1.046×10^{-3}	4.495×10^{-3}	1.129×10^{-2}	1.165×10^{-2}	2.446×10^{-2}
832.7	8.491×10^{-3}	2.470×10^{-2}	5.079×10^{-2}	0.1116	0.2307
1171.	4.331×10^{-2}	0.1298	0.2748	0.3850	0.4490
1696.	0.1731	0.3447	0.4922	0.5712	0.5900
2549.	0.3629	0.5957	0.7517	0.7941	0.7719
3991.	0.6252	0.9125	1.064	1.077	1.004
4848.	0.7475	1.079	1.243	1.242	1.150
6495.	0.9214	1.379	1.621	1.653	1.518
10898.	1.484	2.100	2.357	2.296	2.075
18695.	2.418	3.234	3.451	3.241	2.835
20917.	2.638	3.499	3.711	3.450	3.006
32545.	3.792	4.795	4.884	4.425	3.762

[a] Geopotential altitude in feet is converted from atmospheric depth in g/cm^2 using ref. 8.

Table 2. Conversion factors *(k, k')* and characteristic rigidities for measurements in GOES-10 and GOES-11 proton channels (3)

Channel	Conversion Factor k [a]	Conversion Factor k' [b]	Characteristic Rigidity, MV [c]
P4	4.64	22.25	225.1
P5	15.5	43.04	338.2
P6	90.	252.8	563.9
P7	300.	1210.	950.0
P10	162.	175.6	1225.
P11	1565.	1103.	1700.

[a] k: counts/(particles/cm^2/steradian/MeV)

[b] k': counts/(particles/cm^2/steradian/MV)

[c] When calculating a spectral hardness index, a single rigidity value, called the characteristic rigidity, is assigned to the entire channel.

Table 3. Spectral hardness index correction factors (s) for differential fluxes derived from measurements in GOES-10 and GOES-11 proton channels (3) [a]

γ	P4	P5	P6	P7	P10
0	1.0000	1.0000	1.0000	1.0000	1.0000
1	0.9565	0.9775	0.9733	0.9300	0.9968
2	0.8777	0.9350	0.9233	0.8050	0.9904
3	0.7751	0.8764	0.8553	0.6502	0.9808
4	0.6609	0.8060	0.7753	0.4913	0.9683
5	0.5458	0.7284	0.6888	0.3485	0.9529
6	0.4380	0.6476	0.6011	0.2329	0.9348
7	0.3428	0.5674	0.5161	0.1473	0.9142
8	0.2623	0.4904	0.4366	0.08856	0.8914
9	0.1969	0.4186	0.3645	0.05089	0.8666
10	0.1453	0.3533	0.3006	0.02811	0.8400

[a] Intermediate correction factors are obtained by linear interpolation.

Table 4. Lower and upper rigidity limits associated with parameters α and γ calculated for each channel.

	P4	P5	P6	P7	P10	P11
Lower Rigidity	137	338	564	950	1225	1343
Upper Rigidity	338	564	950	1225	1343	See Step 8